

Temperature effects in the mechanical desorption of an infinitely long lattice chain: Re-entrant phase diagrams

A. M. Skvortsov,¹ L. I. Klushin,² G. J. Fleer,³ and F. A. M. Leermakers^{3,a)}

¹Chemical-Pharmaceutical Academy, Prof. Popova 14, 197022 St. Petersburg, Russia

²Department of Physics, American University of Beirut, Beirut, Lebanon

³Laboratory of Physical Chemistry and Colloid Science, Wageningen University, Dreijenplein 6, 6703 HB Wageningen, The Netherlands

(Received 11 January 2009; accepted 10 March 2009; published online 1 May 2009)

We consider the mechanical desorption of an infinitely long lattice polymer chain tethered at one end to an adsorbing surface. The external force is applied to the free end of the chain and is normal to the surface. There is a critical value of the desorption force f_{tr} at which the chain desorbs in a first-order phase transition. We present the phase diagram for mechanical desorption with exact analytical solutions for the detachment curve: the dependence of f_{tr} on the adsorption energy ε (at fixed temperature T) and on T (at fixed ε). For most lattice models $f_{tr}(T)$ displays a maximum. This implies that at some given force the chain is adsorbed in a certain temperature window and desorbed outside it: the stretched state is re-entered at low temperature. We also discuss the energy and heat capacity as a function of T ; these quantities display a jump at the transition(s). We analyze short-range and long-range excluded-volume effects on the detachment curve $f_{tr}(T)$. For short-range effects (local stiffness), the maximum value of f_{tr} decreases with stiffness, and the force interval where re-entrance occurs become narrower for stiffer chains. For long-range excluded-volume effects we propose a scaling $f_{tr} \sim T^{1-\nu}(T_c - T)^{\nu/\phi}$ around the critical temperature T_c , where $\nu = 0.588$ is the Flory exponent and $\phi \approx 0.5$ the crossover exponent, and we estimated the amplitude. We compare our results for a model where immediate step reversals are forbidden with recent self-avoiding walk simulations. We conclude that re-entrance is the general situation for lattice models. Only for a zigzag lattice model (where both forward and back steps are forbidden) is the coexistence curve $f_{tr}(T)$ monotonic, so that there is no re-entrance. © 2009 American Institute of Physics. [DOI: 10.1063/1.3110604]

I. INTRODUCTION

The study of polymer adsorption from a solution onto a solid surface has a long history and is important for many applications such as adhesion, coating of surfaces, wetting, adsorption chromatography, etc. A fundamental issue is the adsorption-desorption transition of an isolated long polymer chain. There is an important analogy with the melting transition of a double-stranded DNA. Indeed, the conformational features in these two cases are similar, consisting of an alternation of trains (or native helix pieces) and single (or double) loops.

Melting of a double-stranded DNA as well as desorption of an adsorbed chain can be induced by changing the pH or temperature of the solution. For the simplest models of DNA without excluded-volume interactions thermal melting is a second-order phase transition, the same as the adsorption-desorption transition.¹

In contrast to thermal melting, DNA replication *in vivo* is initiated by unzipping of the double-stranded DNA by special enzymes (helicase, polymerase, etc.) which open up the DNA, thereby forming a Y-shaped structure.² It was predicted theoretically that the unzipping of DNA occurs as a first-order transition when the force exceeds a critical value

which depends on temperature.³ Experimentally, the force required to unzip DNA has been measured (typical forces are in the range of 10–15 pN) and the unzipping has been called *directional* or *mechanical melting*.⁴ A similar effect of *mechanical desorption* of a polymer chain was considered theoretically and classified as a first-order phase transition.⁵ Here we see again the close analogy between force-induced polymer desorption and DNA unzipping: in both cases there is a competition between a binding potential and an external stretching force.

Mechanical desorption in experiment can be realized by retracting one end of a polymer chain attached to an atomic force microscopy (AFM) tip. The critical value of the force depends on the nature of the three components polymer/solvent/surface. It was found that a typical desorbing force for a polyacrylic acid chain at cationic, hydrophobic and metallic substrates is ~ 70 pN.⁶

An analytical theory of mechanical desorption was constructed a long time ago for an ideal lattice model⁷ in the limit $N \rightarrow \infty$, and later for a continuum model with finite chain length.^{8–10} Both theories predict the critical desorption force as a function of the adsorption interaction parameter and demonstrate a first-order force-induced conformational phase transition. These theories were formulated in terms of two dimensionless parameters: $u = f\ell/kT$ (where f is the force, ℓ the step length, T the temperature, and k the

^{a)}Electronic mail: frans.leermakers@wur.nl.

Boltzmann constant) and $\chi = \varepsilon/kT$ (where ε is the adsorption energy per segment). Both u and χ depend on T , but the temperature as an independent parameter was never considered in these theories. In the continuum model, an adsorption parameter c was introduced as the inverse extrapolation length, which also did not contain the temperature explicitly.

Monte Carlo (MC) simulations of adsorbing chains in the presence of an end force were performed for interacting self-avoiding chains and a phase diagram was constructed in the three-dimensional parameter space that included the reduced monomer-surface interaction χ , a reduced monomer-monomer attraction, and the reduced force u . In the absence of a force the transitions (adsorption, globulization, and wetting, induced by competition between different interactions) were found to be continuous,^{11,12} whereas the force-induced transitions are first order.

Temperature effects in mechanical desorption were studied by direct enumeration methods for self-avoiding walks on simple square and cubic lattices by Mishra *et al.*¹³ Data for short chains with N up to 20–30 segments were analyzed, and several extrapolation procedures were employed. The phase diagram is defined by the detachment curve, which represents the dependence of the critical desorption force on the temperature, at fixed adsorption energy ε . It was shown that in two dimensions, where the adsorbing surface is replaced by a line, the force f_{tr} at the adsorption/desorption transition increases monotonically as the temperature is lowered and it becomes constant at low temperatures. However, $f_{tr}(T)$ in three dimensions goes through a maximum as the temperature varies so that the phase diagram in the (T, f) plane is re-entrant: at low T the stretched state is re-entered. Similar data for longer chains (up to $N=256$) were obtained by Krawczyk *et al.*¹¹ It was demonstrated also that the distribution curves for the height of the free end have a unimodal form at any external force.

For a semiflexible chain, the problem was analyzed using a combination of scaling analysis and MC simulation,¹⁴ and the re-entrance effect (although quite marginal) was also observed.

In a different study,¹⁵ the dependence of the critical desorption force on temperature was investigated analytically for directed-walk models in two and three dimensions. Different classes of directed walks were considered in two dimensions, all leading to a monotonic decrease in the desorption force with increasing temperature. In three dimensions the phase diagram is re-entrant. Qualitatively similar re-entrant phase diagrams have been obtained in directed models of the mechanical denaturation of double-stranded DNA.¹⁶ Although directed walks are quite useful as theoretical models that allow analytical solutions, their inherent anisotropy may introduce uncontrolled effects that do not exist in real polymers in the absence of additional orienting fields.

Historically the adsorption of a flexible polymer chain on a solid surface was described by ideal random walks on regular lattices.^{17–19} These models allow exact analytical solutions for the partition function in the limit of very long chains, and predict a second-order adsorption/desorption transition that falls entirely within the mean-field picture, including a finite jump in the heat capacity and a linear

growth of the order parameter (the fraction θ of adsorbed segments) just below the transition temperature: $\theta \sim T_c - T$. For a Gaussian chain the dependence of the average number m of surface contacts on the chain length N at $T=T_c$ is $m(T_c) \sim N^{1/2}$. Consequently, the order parameter scales as $\theta(T_c) \sim N^{-1/2}$ at the critical point. In a more general picture that takes into account excluded-volume interactions the chain-length dependence of the average contact number at the critical point is given by the scaling law $m(T_c) \sim N^\phi$, where ϕ is the crossover exponent, which may differ from $\frac{1}{2}$.

Great efforts were put into understanding excluded-volume effects in the adsorption transition. Scaling theory proposed by de Gennes²⁰ predicted that the growth of the order parameter below the transition temperature is related only to the crossover index: $\theta \sim |T_c - T|^{1/\phi-1}$. It follows that the near-critical behavior of standard thermodynamic quantities such as energy and heat capacity in the thermodynamic limit is entirely determined by the value of ϕ . This is in contrast to the geometric properties, such as components of the gyration tensor, etc., which are governed by the Flory indices ν (in three or two dimensions) for the desorbed and adsorbed states, respectively. From a theoretical point of view, the mean-field value $\phi=1/2$ applies to higher-dimensional spaces with $d \geq 4$ where excluded-volume effects are negligible. On the other hand, a conformal-invariance approach²¹ in two dimensions also gives, rather unexpectedly, exactly the value $\phi=1/2$. Various versions of renormalization group calculations in three-dimensional ($3d$) space produce values in the range between $\phi=0.483$ (Ref. 22) and $\phi=0.52$.^{22,23}

MC simulations are routinely made on regular lattices, the simple cubic lattice being one of the most popular. Extensive numerical work using a chain growth Monte Carlo algorithm [pruned-enriched Rosenbluth method for self-avoiding walks (SAW) next to an adsorbing surface] for N up to 8000 and massive statistics produced the estimate $\phi = 0.484 \pm 0.002$,²⁴ although some other authors obtained the estimates $\phi = 0.530 \pm 0.007$ (Ref. 25) and $\phi = 0.54 \pm 0.01$,²⁶ using other versions of MC algorithms and other methods of analysis for the same lattice model. Yet another MC simulation of an off-lattice model with N up to 512 demonstrated that the heat capacity extrapolated to $N \rightarrow \infty$ experiences a finite jump which is consistent with the mean-field value $\phi = 1/2$.²⁷

We summarize that the exponent ϕ is close to 0.5 although the exact value is still being debated. Very importantly, this means that adsorption of real self-avoiding polymers is to a large extent described by ideal chain models, at least as far as thermodynamic properties are concerned. Quantitatively, excluded-volume effects lead to a shift in the transition point and a change in the numerical values of the entropy of the strongly adsorbed state, but these effects are of the same nature as the difference between various lattice types.

In this paper we construct the phase diagram for infinitely long ideal chains on a simple cubic lattice and we demonstrate the origin of the re-entrance effect when the temperature is treated as an independent variable. We study the temperature dependence of average chain characteristics,

such as the order parameter, the energy and the heat capacity per segment for different cross sections of the phase diagram. We also show how to extend the theory to a whole class of ideal lattice chains, most of which have a re-entrant phase diagram. Only in very special cases is the re-entrance effect absent.

This present paper is organized as follows. In Sec. II we consider phase diagrams for mechanical desorption by comparing the free energy of the adsorbed state with that of the stretched state subject to an applied force. We do that first in the coordinates $\chi = \varepsilon/kT$ and $u = f\ell/kT$, and then we consider the temperature dependence explicitly and present the diagram in the variables kT/ε and $f\ell/\varepsilon$. In Sec. III we discuss some average chain properties in each of the two states (adsorbed and stretched), and we investigate the temperature dependence of several thermodynamic properties at a constant external force, in particular when re-entrance occurs. In Sec. IV we generalize to a broader class of lattice models accounting for local excluded-volume effects, and we show that re-entrant behavior persists. We also present a scaling description of long-range excluded-volume effects on the phase diagram and compare it to simulation data found in literature. In Sec. V we discuss an analytical theory for stiffness effects on the detachment curve. In Sec. VI we consider a particular lattice model (zigzag chain) without re-entrance. In Appendixes A–C we derive expressions for the adsorption and stretching free energy of lattice chains, including stiffness effects.

II. PHASE DIAGRAM FOR ADSORBED AND STRETCHED STATES

In this section we present phase diagrams for mechanical desorption both in (χ, u) and in (T, f) coordinates. The coexistence curve $u(\chi)$ is monotonic and it approaches a straight line at strong adsorption. The intercept of this line is related to the entropy of a completely adsorbed (2d) chain. However, the coexistence curve $f(T)$ is nonmonotonic. In a certain force interval and with decreasing temperature the polymer chain is first desorbed (stretched), then adsorbed in some temperature window, and then desorbed again.

A. (χ, u) phase diagram

A standard model for describing the adsorption of a polymer chain is a random walk on a regular lattice. For an end-attached chain the walk starts from the surface. The interaction of each step with the surface is described by a square-well potential with a depth ε and a width ℓ ; here ε is the adsorption energy and ℓ is the step length. Usually, the energy and free energy are measured in kT units, which is convenient when the temperature is constant. The dimensionless adsorption energy parameter χ is defined as $\chi = \varepsilon/kT$.

The free energy of an infinitely long end-attached ideal lattice chain can be obtained analytically. For a six-choice cubic lattice (with five choices for a step starting from the surface) the reduced chemical potential (the free energy per step) $\tilde{\mu}_{\text{ads}} = \mu_{\text{ads}}/kT$ was obtained by Rubin¹⁷ (for a derivation, see Appendix A):

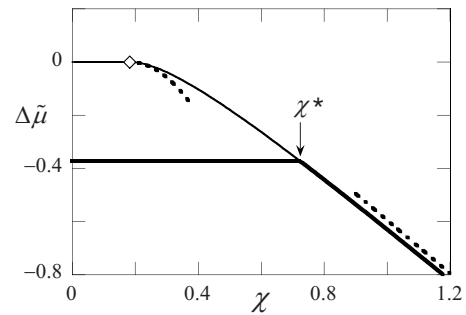


FIG. 1. The free energy per step $\Delta\tilde{\mu}_{\text{ads}}$ (thin solid curve) of an adsorbed chain with respect to a free coil as a function of the adsorption energy parameter χ according to Eq. (1). The diamond is the critical point, the dotted curves are the asymptotes of Eq. (2). The thick solid curve is the free energy $\Delta\tilde{\mu}(\chi, u)$ of an adsorbed chain in the presence of a force $u=1.5$ [Eq. (3)]. The chain is stretched for $\chi < \chi^*$ and adsorbed for $\chi > \chi^*$.

$$\tilde{\mu}_{\text{ads}}(\chi) = \begin{cases} \tilde{\mu}_0, & \chi \leq \chi_c, \\ \ln\left(\frac{e^\chi - 1}{e^\chi} \left[\sqrt{3 + \frac{e^\chi}{e^\chi - 1}} - 2 \right]\right), & \chi \geq \chi_c, \end{cases} \quad (1)$$

$$\chi_c = \ln(6/5) \approx 0.182.$$

Here $\tilde{\mu}_0 = -\ln 6$ is the reduced chemical potential for a free coil where each step has six choices, and the reference state for $\tilde{\mu}$ is a rod, which has zero entropy. We also define $\Delta\mu_{\text{ads}} \equiv \mu_{\text{ads}} - \mu_0$ as the free energy difference between an adsorbed and a free coil. Clearly, $\Delta\mu_{\text{ads}} = 0$ for $\chi < \chi_c$, where $\chi_c = \ln(6/5)$ is the critical value separating the adsorption regime from the desorption regime.

Figure 1 (thin solid curve) gives a plot of $\Delta\tilde{\mu}_{\text{ads}}$ as a function of χ . The diamond on this curve is the critical point. The asymptotes of $\Delta\tilde{\mu}_{\text{ads}}$ in the adsorption regime are shown as the dotted curves. They are given by

$$\tilde{\mu}_{\text{ads}} \approx \begin{cases} -(25/6)(\chi - \chi_c)^2 - \ln 6, & \chi \approx \chi_c, \\ -\chi - \ln 4, & \chi \gg \chi_c. \end{cases} \quad (2)$$

The term $\ln 4$ is the entropy of a flat 2d chain (with four choices per step) in the strong adsorption limit.

Next we consider the effect of a force f applied to the free end of the chain in the direction normal to the surface. Such a force gives rise to a stretching energy $-f\ell$ per step in the direction of the force. We express $f\ell$ again in kT units and define a parameter $u = f\ell/kT$ as the ratio between the stretching energy and the thermal energy. In general, the chemical potential μ depends on both χ and u . According to general principles,

$$\mu(\chi, u) = \min[\mu_{\text{ads}}(\chi), \mu_{\text{str}}(u)]. \quad (3)$$

In Appendix A it is shown that for long chains the free energy $\mu_{\text{str}}(u)$ of a stretched tail is independent of the adsorption energy, and can be deduced from stretching a free coil, as described below.

On a simple cubic lattice there are four orientations parallel to the surface with a statistical weight unity (here the force has no effect), one orientation along the force field with weight e^u , and one orientation opposite to the field with

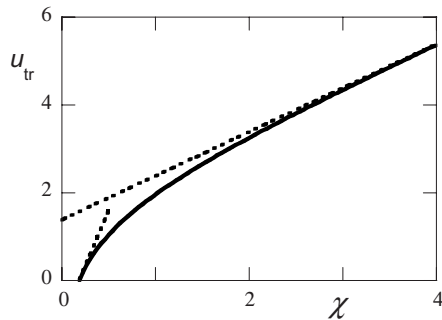


FIG. 2. Phase diagram for mechanical desorption of an ideal lattice chain in the coordinates $\chi = \varepsilon/kT$ and $u = f\ell/kT$. The solid curve is Eq. (5), the dotted lines are its asymptotes. The intercept of the high- χ asymptote is $S_{\text{ads}} = \ln 4$.

weight e^{-u} . Therefore, the partition function Q_{str} in the presence of a force is $Q_{\text{str}} = (4 + e^u + e^{-u})^N = (4 + 2 \cosh u)^N$. The corresponding free energy of stretching per step (with respect to a rod) is given by $\tilde{\mu}_{\text{str}} = -N^{-1} \ln Q_{\text{str}}$ or

$$\tilde{\mu}_{\text{str}}(u) = -\ln(4 + 2 \cosh u) \approx \begin{cases} -u^2/6 - \ln 6, & u \ll 1, \\ -u, & u \gg 1. \end{cases} \quad (4)$$

In the absence of a force μ_{str} equals μ_0 . Some more background on this equation is given in Appendixes A and B.

The thick curve in Fig. 1 shows the free energy $\Delta\tilde{\mu}(\chi, u)$ according to Eq. (3) at $u = 1.5$. For $\chi < \chi^*$ (with $\chi^* = 0.732$ in this example) this force is sufficient to detach the chain and the desorbed stretched chain is stable. For $\chi > \chi^*$ the chain remains adsorbed and is not affected by the force.

The condition $\mu_{\text{ads}}(\chi) = \mu_{\text{str}}(u)$ defines the detachment curve $u_{\text{tr}}(\chi)$ where the adsorbed and stretched states coexist. From Eqs. (1) and (4) the detachment (coexistence) curve $u_{\text{tr}}(\chi)$ is found as

$$u_{\text{tr}} = -\ln\left(\sqrt{3 + \frac{e^\chi}{e^\chi - 1}} - 2\right) \approx \begin{cases} 5(\chi - \chi_c), & \chi \approx \chi_c, \\ \chi + \ln 4, & \chi \gg \chi_c. \end{cases} \quad (5)$$

Equation (5) was obtained more than 30 years ago.²⁸

Figure 2 gives the phase diagram for the mechanical desorption of an adsorbed lattice chain. The region above the detachment curve (solid curve) corresponds to desorbed stretched state, the region below the curve to the adsorbed state. The low- χ and high- χ asymptotes of the detachment curve are indicated as the dotted lines.

In the strong adsorption limit the linear asymptotic form of the coexistence line has a simple physical interpretation. Following the argument of Mishra *et al.*¹³ we write the reduced chemical potential of the (fully) adsorbed chain as $\tilde{\mu}_{\text{ads}}(\chi) = -\chi - S_{\text{ads}}$ and the chemical potential of the (completely) stretched chain as $\tilde{\mu}_{\text{str}}(u) = -u$ since the entropy of the fully stretched state is zero. This leads to the straight line equation $u_{\text{tr}} = \chi + S_{\text{ads}}$ with unit slope and intercept S_{ads} , the entropy of the fully adsorbed state. For a simple cubic lattice $S_{\text{ads}} = \ln 4$ and the intercept is positive.

It is clear from Fig. 2 that in the coordinates (χ, u) the coexistence curve is monotonic. We show below that re-entrant behavior appears when the temperature is treated as an independent variable.

B. Force-temperature phase diagram

So far we used χ and u as the control parameters. Both are inversely proportional to the temperature. The same applies to the reduced free energies $\tilde{\mu}_{\text{ads}}$ and $\tilde{\mu}_{\text{str}}$. The yardstick was the thermal energy kT .

In the remainder of this paper we concentrate on the temperature dependence. Hence, we keep the adsorption energy ε constant, and we vary χ by changing the temperature. It is then convenient to express all (free) energies in units ε : $\mu/\varepsilon = (kT/\varepsilon)\tilde{\mu}$, $f\ell/\varepsilon = (kT/\varepsilon)u$, and $kT/\varepsilon = 1/\chi$. It would be possible to set $k = \ell = \varepsilon = 1$ in these expressions, which amounts to redefining T and f as dimensionless quantities. We prefer to distinguish between real and dimensionless temperature, and between real and dimensionless force. We therefore define the dimensionless quantities

$$\boldsymbol{\mu} \equiv \mu/\varepsilon, \quad \boldsymbol{f} \equiv f\ell/\varepsilon, \quad (6)$$

$$\boldsymbol{T} \equiv kT/\varepsilon = 1/\chi, \quad \boldsymbol{T}_c = 1/\chi_c = 5.485,$$

where the bold-face symbol indicates that ε is the yardstick. Clearly, the real chemical potential μ is obtained by multiplying $\boldsymbol{\mu}$ by ε , the real force f by multiplying \boldsymbol{f} by ε/ℓ , and the real temperature T by multiplying \boldsymbol{T} by ε/k . We assume that ε is strictly enthalpic and we ignore the “hidden” temperature dependence in, e.g., bond length, bond angles, etc. In an experimental system ε might contain an entropic contribution so that it becomes temperature dependent. However, experimental determination of ε is very difficult. In this paper we avoid these complications and assume constant ε throughout. The relation between $\boldsymbol{\mu}$ and \boldsymbol{f} (units ε) and $\tilde{\mu}$ and u (units kT) is simply $\boldsymbol{\mu} = \boldsymbol{T}\tilde{\mu}$ and $\boldsymbol{f} = \boldsymbol{T}u$. The critical temperature \boldsymbol{T}_c depends on the lattice type; the value given is for a six-choice cubic lattice. Adsorption occurs only for $\boldsymbol{T} < \boldsymbol{T}_c$.

Equations (1), (4), and (5) are rewritten with χ replaced by $1/\boldsymbol{T}$, u by $\boldsymbol{f}/\boldsymbol{T}$, and $\tilde{\mu}$ by $\boldsymbol{\mu}/\boldsymbol{T}$. The chemical potential of an adsorbed chain [Eq. (1)] in the absence of a force is

$$\boldsymbol{\mu}_{\text{ads}} = \begin{cases} \boldsymbol{\mu}_0 = -\boldsymbol{T} \ln 6, & \boldsymbol{T} \geq \boldsymbol{T}_c, \\ \boldsymbol{T} \ln((1 - e^{-1/\boldsymbol{T}})(\sqrt{3 + 1/(1 - e^{-1/\boldsymbol{T}})} - 2)), & \boldsymbol{T} \leq \boldsymbol{T}_c. \end{cases} \quad (7)$$

The asymptotes in the adsorption regime $\boldsymbol{T} < \boldsymbol{T}_c$ are

$$\boldsymbol{\mu}_{\text{ads}} \approx \begin{cases} -(25/6\boldsymbol{T}_c)(1 - \boldsymbol{T}/\boldsymbol{T}_c)^2 - \boldsymbol{T} \ln 6, & \boldsymbol{T} \approx \boldsymbol{T}_c, \\ -1 - \boldsymbol{T} \ln 4, & \boldsymbol{T} \ll \boldsymbol{T}_c. \end{cases} \quad (8)$$

The quadratic dependence $\boldsymbol{\mu}_{\text{ads}} \sim (\boldsymbol{T}_c - \boldsymbol{T})^2$ shows that the adsorption of an ideal chain displays a second-order phase transition.

The free energy of stretching as a function of T is found from Eq. (4):

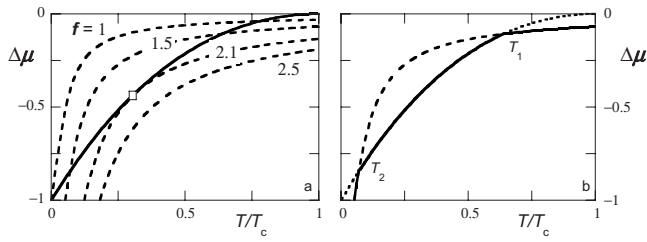


FIG. 3. (a) Chemical potentials $\Delta\mu_{\text{ads}}$ (solid curve) and $\Delta\mu_{\text{str}}$ (dashed) as a function of temperature. The dashed curves for $\Delta\mu_{\text{str}}$ are given for $f=1$ (top), 1.5, 2.098, and 2.5 (bottom). The square is the point where, at $f=f^*=2.098$ and $T^*/T_c=0.308$, $\Delta\mu_{\text{ads}}$ and $\Delta\mu_{\text{str}}$ just touch. (b) The situation at $f=1.5$. The equilibrium states $\Delta\mu(T)$ with the lowest free energy are indicated as the thick solid curve, with kinks at the transition temperatures T_1 and T_2 , the unstable states are dotted ($\Delta\mu_{\text{ads}}$) or dashed ($\Delta\mu_{\text{str}}$).

$$\mu_{\text{str}} = -T \ln[4 + 2 \cosh(f/T)]$$

$$\approx \begin{cases} -f^2/6T - T \ln 6, & f/T \ll 1, \\ -f, & f/T \gg 1. \end{cases} \quad (9)$$

The low- T limit for μ_{str} is the energy $E_{\text{str}} = -f\ell$ for the fully stretched state: $\mu_{\text{str}} = -f\ell$ or $\mu_{\text{str}} = -f$.

Figure 3(a) (solid curve) shows $\mu_{\text{ads}} = \mu_{\text{ads}} - \mu_0$ as a function of temperature; its low- T limit is $\Delta\mu_{\text{ads}} = -f + T \ln(6/4)$. The dashed curves in Fig. 3(a) give $\Delta\mu_{\text{str}} = \mu_{\text{str}} - \mu_0$ as a function of T for four values of f . For $T \rightarrow 0$, $\Delta\mu_{\text{str}}$ equals $-f + T \ln 6$.

For a low force ($f=1$ or below) the curves for μ_{ads} and μ_{str} intersect once: at high T the stretched state is stable, at low T the chain remains adsorbed. For a high force [$f=2.5$ in Fig. 3(a)] the curves do not intersect: $\mu_{\text{str}} < \mu_{\text{ads}}$ at any temperature and the chain is always stretched. In an intermediate force interval there are two intersections and, consequently, the stretched state is re-entered at low T .

The square in Fig. 3(a) corresponds to the situation that the curves for μ_{str} and μ_{ads} just touch without intersecting; this happens for a particular value $f=f^*=2.098$ at $T^*/T_c=0.308$. The force interval where the curves intersect twice is thus $1 < f < f^*$; then there is a temperature window in which the chain is adsorbed, and there is re-entrance of the stretched state at low T .

The equilibrium free energy for $f=1.5$ is indicated in Fig. 3(b) as the solid curve with kinks at $T_1 (=0.640T_c)$ and $T_2 (=0.069T_c)$. At the transition temperatures T_1 and T_2 the slope $\partial\mu/\partial T$ is discontinuous. Consequently, the entropy and energy show a jump (see also Figs. 9 and 10) and the transition is first order.

The detachment curve follows from Eq. (5) as

$$f_{\text{tr}} = -T \ln(\sqrt{3 + 1/(1 - e^{-1/T})} - 2)$$

$$\approx \begin{cases} 5(1 - T/T_c)\sqrt{T/T_c}, & T \approx T_c, \\ 1 + T \ln 4, & T \ll T_c. \end{cases} \quad (10)$$

The value $f=1$ for $T=0$ originates from $\mu_{\text{ads}} = -\varepsilon$ and $\mu_{\text{str}} = -f\ell$, so $f\ell = \varepsilon$ or $f=1$.

A plot of f_{tr} as a function of T is given in Fig. 4, together with the two asymptotes of Eq. (10). The region below the

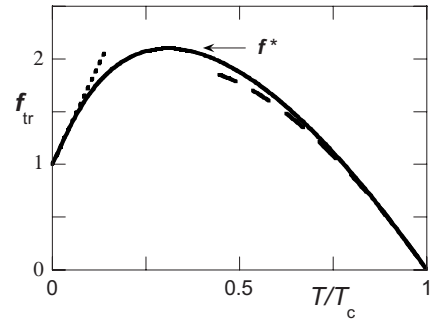


FIG. 4. Phase diagram for an ideal lattice chain in $f(T)$ coordinates. The solid curve is the detachment curve [Eq. (10)]. The low- T asymptote (dotted) and high- T asymptote (dashed) are also indicated. In the region $1 < f < f^*$ a horizontal line (i.e., constant force) intersects the solid curve twice, so there is re-entrance of the stretched state at low T .

solid curve is the adsorption region, and above this curve the chain is desorbed. The top of the curve is f^* at T^* , which corresponds to the square in Fig. 3(a).

A horizontal line for a constant force $f > f^*$ does not intersect the detachment curve in Fig. 4: for such a high force the chain is desorbed at any T . For a low force $f < 1$ there is one intersection: desorption for $T > T_1$, adsorption for $T < T_1$. In the intermediate force interval $1 < f < f^*$ there are two intersections: now there is detachment at high and low temperature, and the chain remains adsorbed in a window $T_1 > T > T_2$.

The low- T limit of the coexistence line corresponds to strong adsorption. In this limit $f_{\text{tr}}\ell \approx \varepsilon + TS_{\text{ads}}$ or, in reduced form, $f_{\text{tr}} = 1 + T \ln 4$, and f_{tr} increases linearly with increasing T . On the other hand, the coexistence line decreases linearly to zero as T approaches the critical temperature T_c . Because of the different sign of the slope $\partial f_{\text{tr}}/\partial T$ at both extremes, there must be an intermediate maximum and, consequently, re-entrance. The re-entrance behavior in a (T, f) diagram is directly related to the positive intercept of the strong adsorption asymptote in the coordinates (χ, u) , see Fig. 2 and its discussion.

III. AVERAGE PROPERTIES

We consider several chain properties (adsorbed fraction, average stretching, energy, and heat capacity) as a function of temperature at a fixed force. This corresponds to making horizontal cross sections through the (T, f) phase diagram. We first describe the temperature effects in each of the two phases, regardless of which phase is the stable one. Then we refine the picture by selecting for each temperature only the thermodynamically stable phase with the lowest chemical potential.

A. Pure adsorbed and stretched states

The average fraction of adsorbed segments is $\theta = -\partial\tilde{\mu}_{\text{ads}}/\partial\chi$, where $\tilde{\mu}_{\text{ads}}$ is given by Eq. (2). The result (first derived by Rubin¹⁷) may be written as

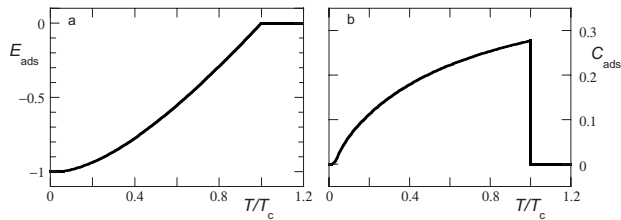


FIG. 5. The energy E_{ads} (a) and heat capacity C_{ads} (b) for the adsorbed state as a function of T . At $T=T_c$ the slope $\partial E/\partial T$ is discontinuous; consequently C_{ads} shows a jump at $T=T_c$.

$$\theta = \begin{cases} 0, & T \geq T_c, \\ 1 - \frac{p}{2} + \frac{p}{\sqrt{3+p}}, & T \leq T_c, \end{cases} \quad (11)$$

where $p=1/(1-e^{-1/T})$ is a function of temperature. A plot of $\theta(T)$ is given later (Fig. 7). At $T=T_c$ the curve $\theta(T)$ has a discontinuity in slope, which leads to a jump in the heat capacity as discussed below.

The energy of the adsorbed state is simply $E_{\text{ads}}=-\theta$, where E is in units ε . The entropy (in units k) is given by $TS_{\text{ads}}=E_{\text{ads}}-\mu_{\text{ads}}$. The heat capacity C (also in units k) is $\partial E/\partial T$:

$$C_{\text{ads}} = \begin{cases} 0, & T \geq T_c, \\ \frac{1}{T^2} p(p-1) \left[\frac{1}{2} - \frac{3+p/2}{(3+p)^{3/2}} \right], & T < T_c. \end{cases} \quad (12)$$

Figure 5 gives a plot of E_{ads} and C_{ads} as a function of temperature. The energy E_{ads} increases from -1 (ε units) at $T=0$ to zero at $T=T_c$; for $T>T_c$ its value remains zero. The heat capacity C_{ads} is zero at $T=0$ and it increases with T to $(25/3)/T_c^2=0.277$ at $T=T_c$, where it jumps to zero.

We introduce a stretching parameter $\zeta=Z/N$, where Z is the average distance (measured in units ℓ) of the free end from the surface. For an adsorbed chain $\zeta=0$ in the limit of large N , since Z is of order \sqrt{N} or less. In the stretched state the fraction θ of adsorbed segments is zero and the stretching parameter equals $\zeta=-\partial\tilde{\mu}_{\text{str}}/\partial u$ or

$$\zeta = \frac{\sinh(f/T)}{2 + \cosh(f/T)}. \quad (13)$$

A plot of $\zeta(T)$ is given later (Fig. 8). The average stretching energy is $E_{\text{str}}=-f\zeta$ per step. The heat capacity of the stretched state follows as $C_{\text{str}}=(\partial E_{\text{str}}/\partial T)_f$:

$$C_{\text{str}} = \left(\frac{f}{T}\right)^2 \frac{1 + 2 \cosh(f/T)}{(2 + \cosh(f/T))^2}. \quad (14)$$

Figure 6 gives a plot of E_{str} and C_{str} as a function of T , for $f=1$ (solid curves) and $f=2$ (dashed). For very low T , $E_{\text{str}}=-f$ and it increases monotonically with T toward zero at very high T . The heat capacity is zero at both extremes, but it has an intermediate maximum. Since C_{str} is a universal function of f/T , the two curves in Fig. 6(b) differ by a factor of 2 on the temperature scale; they would coincide when an abscissa scale T/f is used.

We note that the thermodynamic quantities shown in Fig. 6 are well known functions of the force at fixed temperature,

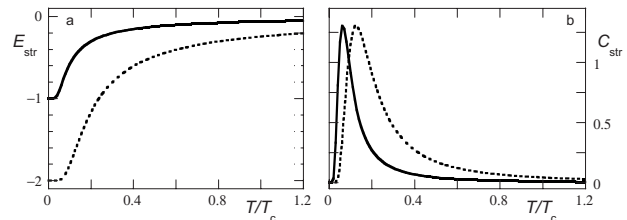


FIG. 6. The energy E_{str} (a) and heat capacity C_{str} (b) for the stretched state as a function of T . The curves are given for two forces: $f=1$ (solid) and $f=2$ (dotted).

but the temperature effects themselves are not commonly discussed. Increasing the temperature leads to an increase in the elastic modulus of the chain, which results in less stretching and larger entropy. In another language, for a lattice chain at low temperature only one microstate with all bonds oriented along the force field survives, while at high temperatures all six orientations are populated equally. This is the origin of the characteristic Schottky peak in the heat capacity; such a peak is well known for two-state systems.²⁹ For example, a spin $\frac{1}{2}$ carrying a magnetic moment m in a magnetic field H has two energy levels $+mH$ and $-mH$. The heat capacity is $C=(mH/kT)^2/\cosh^2(mH/kT)$ per spin, which gives a similar temperature dependence as in our model.

The question may arise whether this $C_{\text{str}}(T)$ curve could be obtained experimentally. One possibility would be to study polymer networks under large constant load. However, the distribution of subchain lengths in real networks would complicate the total heat capacity curve containing contributions from subchains with different deformation. Note that the low- T behavior, including the peak itself, is model dependent. The simple cubic lattice model considered here obviously ignores low-amplitude fluctuations in the torsion angles of real polymer chains.

B. Adsorbed fraction and stretching degree along constant-force cross sections of the phase diagram

When a large force $f>f^*$ is applied the chain is always stretched and $\theta=0$ at any temperature. In this stretched state $\zeta(T)$ does not depend on the adsorption energy and is a function of T/f only. When the force is in the interval $1<f<f^*$, the chain is desorbed at high temperature, adsorbed in an intermediate temperature window, and again desorbed at low T (re-entrance of the stretched state). This implies that inside the window all thermodynamic properties are given by the equations for the adsorbed state, whereas outside this window the “stretched” versions apply.

Figure 7 shows the dependence $\theta(T)$ for $f=1$ (a) and $f=1.5$ (b). The full discontinuous curves describe the equilibrium states, the dotted sections give $\theta(T)$ in the absence of a force. For $f=1$ the detachment curve in the phase diagram is crossed only once. So there is one transition from stretched (high T) to adsorbed (low T). For $f=1.5$ the detachment curve is crossed twice. Consequently, there is now an adsorption window where the adsorbed state is stable; outside this window the chain is stretched. The window exists only for

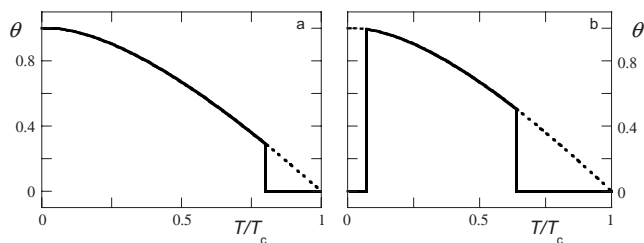


FIG. 7. The fraction θ of adsorbed segments as a function of T when the phase diagram of Fig. 4 is crossed at a constant force. At $f=1$ (a) there is one transition from stretched to adsorbed. At $f=1.5$ (b) there are transitions from stretched to adsorbed and back. The dotted sections represent $\theta(T)$ in the absence of a force.

$1 < f < f^*$, and its width and position depends on the force. Inside the window θ does not depend on the applied force.

Figure 8 shows similar data for the stretching parameter ζ , for $f=1$ (a) and $f=1.5$ and 2.5 (b). For $f=1$ there is again one transition, with $\zeta=0$ in the adsorbed state (low T). For $f=1.5$ we see the same adsorption window as in Fig. 7(b). For $f=2.5$ (which is above f^*) the chain is stretched at any T .

An intriguing situation appears when the cross section in Fig. 4 is a horizontal tangent to the top ($f=f^*$) of the detachment curve in Fig. 4. On the one hand, the adsorption window should degenerate into a single vertical line; on the other hand the coexistence line is never crossed but only touched. The behavior of the thermodynamic quantities in this point is not quite clear and would require further analysis.

C. Energy and heat capacity

In Fig. 9 we show how the energy and heat capacity depend on T for $f=1$, where the detachment curve of Fig. 4 is crossed once. The dotted curve gives E_{str} and C_{str} , the dashed curves are E_{ads} and C_{ads} . The thermodynamic equilibrium is indicated as the solid curve. The energy jumps from E_{ads} to E_{str} and the heat capacity C from C_{ads} to C_{str} . Moreover, because E is discontinuous at the transition temperature, C displays a δ peak.

Figure 10 gives the same situation for $f=1.8$, where the detachment curve of Fig. 4 is crossed twice. Now we see two jumps in both E and C . The heat capacity has two δ peaks because $\partial E / \partial T$ diverges twice.

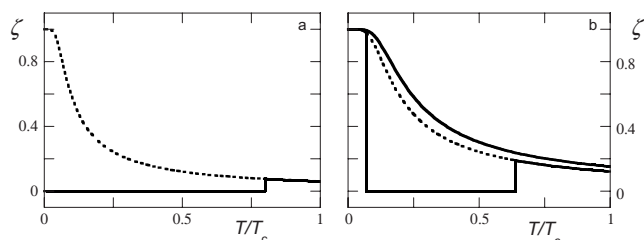


FIG. 8. The stretching parameter ζ as a function of T/T_c when the phase diagram of Fig. 4 is crossed at a constant force: $f=1$ (a), and $f=1.5$ and 2.5 (b). For $f=1$ there is one transition from stretched to adsorbed. For $f=2.5$ (top curve in b) there is no adsorbed state and $\zeta(T)$ is given by Eq. (13) for any T . For $f=1.5$ the adsorption window ($\zeta=0$) is the same as in Fig. 7(b), outside this window the chain is stretched. The unstable stretched sections of $\zeta(T)$ are dotted.

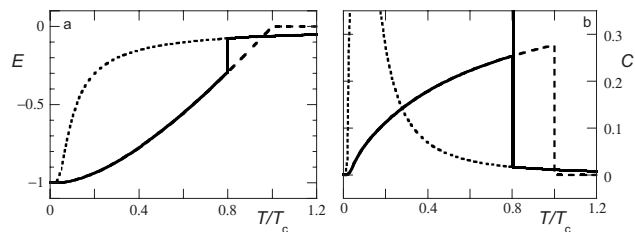


FIG. 9. The energy E (a) and heat capacity C (b) as a function of T/T_c when the coexistence curve in Fig. 4 is crossed at a constant force $f=1$. The dashed parts are for the pure adsorbed state (Fig. 5), the dotted parts for the pure stretched state (Fig. 6). The equilibrium situation is indicated by the solid curves: they show a jump at $T/T_c=0.799$ from stretched to adsorbed, but there is no re-entrance of the stretched state. The heat capacity displays a δ peak.

IV. EXCLUDED-VOLUME EFFECTS

All the results presented so far were based upon an ideal six-choice lattice chain, for which excluded-volume effects are neglected. It is generally understood that these effects can produce both quantitative and qualitative changes in the behavior of polymer systems.³⁰ Excluded-volume effects can be roughly divided into short range and long range. Short-range effects are due to steric repulsion of neighboring monomers. They are model dependent but can be quantitatively quite important. As an example we discuss a five-choice model in which immediate step reversals are forbidden. We compare the results with numerical data of Krawczyk *et al.*¹¹ and Mishra *et al.*¹³ for SAWs on a simple cubic lattice. The former authors used a so-called flat PERM algorithm for chain lengths up to $N=256$; they also extrapolated to $N \rightarrow \infty$. The latter authors calculated the critical desorption force as a function of temperature by exact enumeration for $N \leq 20$, combined with several extrapolation methods (ratio method, Padé analysis, and differential approximations) to estimate the long-chain limit.

Long-range effects are due to interactions between monomers that are quite distant along the chain contour; they lead to model-independent universal behavior which is described by scaling theory. We present such a theory for the force-temperature phase diagram close to the critical temperature T_c .

A. Five-choice model

An exact theory for a random walk without step reversals and with an arbitrary statistical weight g for a forward step (in the direction of the previous step) was developed by Birshtein *et al.*³¹ The general form for the stretching free

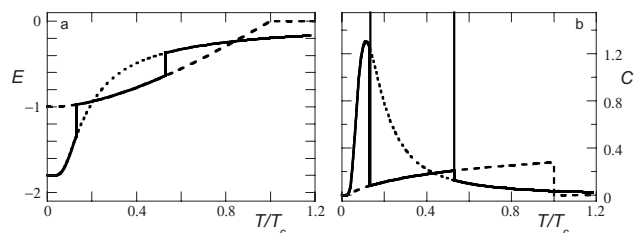


FIG. 10. As Fig. 9 but now for $f=1.8$ where the detachment curve is crossed twice. There are two jumps both in E and C . The heat capacity has two δ peaks.

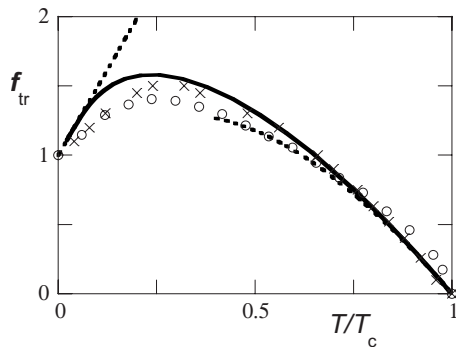


FIG. 11. Phase diagram $f_{tr}(T/T_c)$ for an ideal chain without step reversals (solid curve) and for self-avoiding walks (symbols) on a simple cubic lattice: circles are for $N=256$ (Ref. 11), crosses for $N \rightarrow \infty$ (Ref. 13). The dotted curves are the analytical asymptotes of Eq. (18).

energy is given in Appendix B, and that for the adsorption free energy in Appendix C. A five-choice model for a flexible chain ($g=1$) without step reversal is a special case of these general equations.

The critical value χ_c for arbitrary g is given in Eq. (C5). Upon substituting $g=1$ and converting the energy parameter toward temperature we find

$$1/T_c = \chi_c = \ln(5/4), \quad T_c \approx 4.48 \quad (15)$$

For a five-choice model the free energy of a $3d$ coil is $\mu_0 = -kT \ln 5$ or $\mu_0 = -T \ln 5$, and the free energy of a completely adsorbed $2d$ chain is $\mu_{ads} = -\varepsilon - kT \ln 3$ or $\mu_{ads} = -1 - T \ln 3$. The full analytical expressions for μ_{str} and μ_{ads} are rather complicated, so below we restrict ourselves to the asymptotic forms for $T \approx T_c$ and for low T .

The limits for μ_{ads} are given in Eq. (C6). With $g=1$ and $T=1/\chi$:

$$\mu_{ads} \approx \begin{cases} -(50/9T_c)(1 - T/T_c)^2 - T \ln 5, & T \approx T_c, \\ -1 - T \ln 3, & T \ll T_c. \end{cases} \quad (16)$$

In comparison with Eq. (8) for a six-choice lattice we see a difference in the entropy terms, and a different prefactor of the quadratic term.

The limits for the stretching free energy follow in the same way from Eq. (B11):

$$\mu_{str} = \begin{cases} -f^2/4T - T \ln 5, & f/T \ll 1, \\ -f, & f/T \gg 1. \end{cases} \quad (17)$$

From $\mu_{ads} = \mu_{str}$ we obtain the asymptotes for the transition force:

$$f_{tr} \approx \begin{cases} (10/3)(1 - T/T_c)\sqrt{T/T_c}, & T \approx T_c, \\ 1 + T \ln 3, & T \ll T_c, \end{cases} \quad (18)$$

This form is the same as in Eq. (10) for the six-choice model, with again a different prefactor and a different low- T entropy.

Figure 11 (solid curve) gives f as a function of T/T_c according to Eqs. (B10) and (C1)–(C4), plus the asymptotic forms of Eq. (18). The symbols in these diagrams are the numerical data for SAWs with $\varepsilon=1$, taken from Krawczyk *et al.*¹¹ (circles) for $N=256$ and Mishra *et al.*¹³ (crosses) for

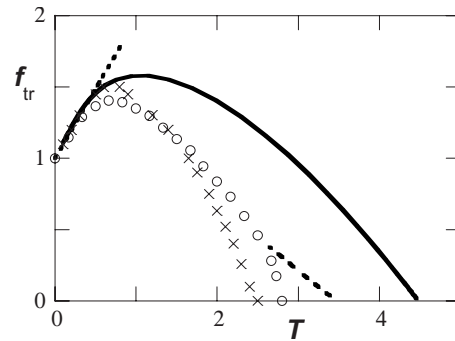


FIG. 12. The phase diagram of Fig. 11 replotted as $f_{tr}(T)$. The dashed curve is the scaling description of Eq. (22), using $T_c=3.496$ (Ref. 37). The low- T asymptote $1+T \ln 2.638$ (Ref. 37) for an SAW on a cubic lattice is also indicated.

$N \rightarrow \infty$ (extrapolated). For obtaining T/T_c from these numerical data we used the estimates $T_c=2.8$ (Ref. 11) and $T_c=2.5$,¹³ which are the temperatures where in the simulations the desorption force vanishes.

The analytical detachment curve has the same shape as in Fig. 4, but the force interval for re-entrance is smaller, because f^* (2.10 for six choice) is smaller (1.58 in Fig. 11). With the coordinates used in this figure the simulation data are rather close to the analytical curve. There is a slight discrepancy at low T , but the detachment force for $T=0$ is the same in all cases. This is because the fully stretched chain has a length $N\ell$ regardless whether the chain is self-avoiding or not. The apparent similarity between simulations and analytical model is somewhat deceptive, although, because of the different values of T_c . We return to this issue in Fig. 12. First we present a scaling theory for long-range excluded-volume effects that describes the high- T branch of the detachment curve for an SAW on a simple cubic lattice provided T_c is accurately known.

B. Scaling description of long-range excluded-volume effects

In order to develop a scaling picture for the mechanical desorption of an adsorbed chain, we have to replace the mean-field exponents used so far by excluded-volume exponents, and we have to find the numerical prefactors. In the introduction we discussed the scaling behavior of the order parameter (adsorbed fraction θ) close to the critical point. This may be immediately translated to the scaling behavior of the adsorption free energy. The free energy per step counted from the free coil in the limit of long chains may be written as

$$\Delta\mu_{ads} \approx 0.57(1 - T/T_c)^{1/\phi}, \quad (19)$$

where ϕ is the crossover index which is close to 0.5, as discussed extensively in Sec. I. The numerical constant 0.57 represents a nonuniversal dimensionless amplitude. We estimated this value from MC data of Vrbová *et al.*³² for an SAW on a simple cubic lattice.

The response of a chain with excluded-volume interactions to stretching by an external force is directly related to the distribution of the end-to-end distance r . The scaling form of this distribution is

$$W(r/r_0) = B_1(r/r_0)^{2+(\gamma-1)/\nu} \exp[-B_2(r/r_0)^{1/(1-\nu)}], \quad (20)$$

where $r_0 = b\ell N^\nu$ is the unperturbed end-to-end distance (with b a model-dependent factor of order unity), ν the Flory exponent, and $\gamma = 1.1575(6)$ the partition function critical exponent.³³ This form was first suggested by Fisher³⁴ and later refined by des Cloiseaux.³⁰ The two numerical coefficients are completely determined by the normalization conditions $\int W(r)dr = 1$ and $\int W(r)rdr = r_0$, which leads to $B_1 = 3.032$ and $B_2 = 1.084$. Although this expression does not follow from any exact theory and is to some extent an interpolation formula with the correct asymptotic behavior, it was extensively tested by simulations³⁵ and proved to be highly accurate. This distribution function contains the free energy of stretching $F/T \approx B_2(r/r_0)^{1/(1-\nu)}$, valid for strong stretching ($r \gg r_0$).

The restoring force $f = \partial F / \partial r \sim (T/r_0)(r/r_0)^{\nu/(1-\nu)}$ follows as the Pincus deformation law.³⁶ It is now possible to calculate the partition function $Q_N(f) = \int \exp[(-F(z) + fz)/T] dz$ in a constant-force ensemble. Employing saddle-point integration one obtains $\Delta\mu_{\text{str}}/T = C(f/T)^{1/\nu}$. The prefactor $C = b^{1/\nu} \nu [(1-\nu)B_2]^{1-1/\nu}$ contains two universal constants (B_2 and ν) and one model-dependent factor $b = r_0/(\ell N^\nu)$; for a simple cubic lattice Grassberger³⁷ found $b = 1.095$. So we obtain

$$\Delta\mu_{\text{str}} = 0.35 T(f/T)^{1/\nu}. \quad (21)$$

Combining Eqs. (19) and (21) we find the asymptotic scaling form for the transition force:

$$f_{\text{tr}} = 1.34 T^{1-\nu}(1 - T/T_c)^{\nu/\phi}. \quad (22)$$

Note that the high- T asymptotes of Eqs. (10) (six choice) and (18) (five choice) follow the same scaling law with the mean-field exponents $\nu = \phi = 0.5$.

Figure 12 replots the data of Fig. 11 as $f(T)$, and gives also the scaling result of Eq. (22), using $\phi = 0.5$ and $T_c = 3.496$. The latter result is due to Hegger and Grassberger³⁸ and seems to be the best estimate available in the literature. Other reported values range from 3.40 to 3.62.^{39,40} For $N = 256$ Krawczyk *et al.*¹¹ found $T_c = 2.8$, but their extrapolation to $N \rightarrow \infty$ gives $T_c = 3.27$. The value 2.5 by Mishra *et al.* deviates considerably from all other estimates. The origin of this discrepancy is probably related to the method of estimating the desorption transition point from the maximum of the heat capacity, which contains large finite-size corrections that are difficult to account for. The Mishra result underestimates the “true” transition temperature by about the same amount as ideal chain theory overestimates it.

Figure 12 gives also the low- T asymptote $f_{\text{tr}} = 1 + TS_{\text{ads}}$, with $S_{\text{ads}} = \ln 2.638 \approx 0.97$ for a 2d SAW on a square lattice.³⁷ This slope is close to that in the analytical theory for a five-choice chain [Eq. (18)], where $S_{\text{ads}} = \ln 3 \approx 1.1$.

V. STIFFNESS EFFECTS ON THE DETACHMENT CURVE

All discussion so far referred to flexible chains where the Kuhn segment length A (in units ℓ) is close to the step length. In this section we investigate stiffness effects. A stiffness parameter g is introduced as the statistical weight for a

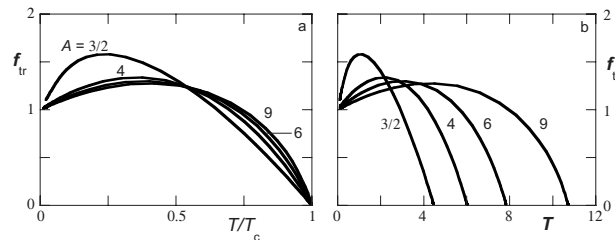


FIG. 13. Effect of chain stiffness on the phase diagram for mechanical desorption. The detachment curve f_{tr} is plotted as a function of T/T_c (a) and as a function of T (b). The value of the Kuhn length is $3/2$, 4, 6, and 9, as indicated.

forward step (i.e., in the direction of the previous step). We assume that the stiffness parameter g is independent of temperature. In principle, the temperature dependence could be included by writing $g = \exp(\Delta U/kT)$ with constant ΔU for the difference in energy between forward and perpendicular steps. However, that would make the already involved equations (see Appendix C) even more complicated. For the sake of simplicity we take constant g , which should give insight in the trends for stiffer chains. In the equations below, we do not use the parameter g but only the Kuhn length A , defined as $A = 1 + g/2$.

According to Eq. (C5) in Appendix C the critical temperature T_c as a function of A is given by

$$1/T_c = \chi_c = \ln \frac{2 + 2/A}{1 + \sqrt{1 + 4/A^2}}. \quad (23)$$

For very stiff chains $\chi_c = 1/A$ and $T_c = A$. The free energy of a 3d coil is $\mu_0 = -kT \ln(2+2A)$ or $\mu_0 = -T \ln(2+2A)$ and the free energy of a 2d adsorbed chain is $\mu_{\text{ads}} = -\epsilon - kT \ln(2A)$ or $\mu_{\text{ads}} = -1 - T \ln(2A)$.

Exact analytical expressions for μ_{str} [Eq. (B10)] and μ_{ads} [Eqs. (C1)–(C4)] are presented in Appendixes B and C. Here we give only the asymptotes. Equation (C6) may be written as

$$\mu_{\text{ads}} \approx \begin{cases} -(B^2/6T_c)(1 - T/T_c)^2 - T \ln(2 + 2A), & T \approx T_c, \\ -1 - T \ln(2A), & T \ll T_c, \end{cases} \quad (24)$$

where $B^2 = A^{-1}(A+1)^2(A^2+4)\exp(-2/T_c)$.

Similarly, the asymptotes of μ_{str} follow from Eq. (B11):

$$\mu_{\text{str}} \approx \begin{cases} -Af^2/6T - T \ln(2 + 2A), & f/T \ll 1, \\ -f - T \ln(2A - 2), & f/T \gg 1. \end{cases} \quad (25)$$

Combining Eqs. (24) and (25) we find the asymptotic behavior of the detachment curve:

$$f_{\text{tr}} \approx \begin{cases} (B/\sqrt{A})(1 - T/T_c)\sqrt{T/T_c}, & T \approx T_c, \\ 1 + T \ln(A/(A-1)), & T \ll T_c. \end{cases} \quad (26)$$

For $A \gg 1$ Eq. (26) simplifies to

$$f_{\text{tr}} \approx \begin{cases} (T_c - T)\sqrt{T/T_c}, & T \approx T_c, \\ 1 + T/A, & T \ll T_c. \end{cases} \quad (27)$$

Figure 13 shows the full detachment curve, calculated according to Appendixes B and C, both in the forms $f(T/T_c)$ (a)

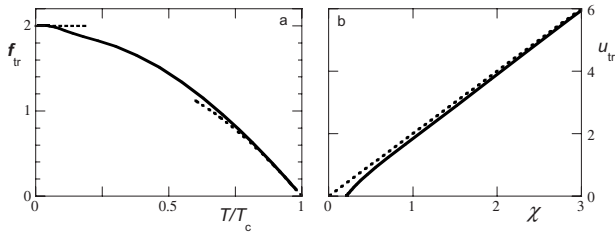


FIG. 14. Phase diagram for a zigzag chain, in both the coordinates $f(T/T_c)$ (a) and $u(\chi)$ (b). The solid curves were calculated from Eqs. (B10) and (C1)–(C4). The dotted curves are the asymptotes [Eq. (31) for (a), 2χ for (b)]. There is no re-entrance in (a), and no intercept in (b).

and in the form $f(T)$ (b), for $A=3/2, 4, 6$, and 9 . There are several aspects in the way in which the detachment curve changes as the chain stiffness is increased. In the limit of large A , $T_c \approx A$, which explains the variation of the critical temperature in Fig. 13(b). The (negative) slope df_{tr}/dT close to the critical point becomes independent of stiffness for large A , as follows from Eq. (27). At the low-temperature end the (positive) slope decreases as $1/A$. As a consequence, the force interval where re-entrance occurs narrows for stiffer chains: the top f^* of the detachment curve decreases with increasing A .

VI. ZIGZAG CHAIN

Finally, we treat a special lattice model where the re-entrance effect is absent: a zigzag chain. We define a zigzag chain as a restricted walk on a simple cubic lattice where both forward and back steps are forbidden: at each step the chain has to make a 90° turn. This corresponds to the limit $g=0, A=1$ of the general expressions given in Appendixes B and C.

The critical temperature follows from Eq. (23):

$$1/T_c = \chi_c = \ln(\sqrt{5} - 1), \quad T_c \approx 4.72. \quad (28)$$

For a zigzag chain the free energy of a $3d$ coil is $\mu_0 = -kT \ln 4$ or $\mu_0 = -T \ln 4$, and the free energy of a $2d$ chain is $\mu_{ads} = -\varepsilon - kT \ln 2$ or $\mu_{ads} = -1 - T \ln 2$. The asymptotic forms for μ_{ads} are a special case of Eq. (24):

$$\mu_{ads} \approx \begin{cases} -((5 + \sqrt{5})^2/24T_c)(1 - T/T_c)^2 - T \ln 4, & T \approx T_c \\ -1 - T \ln 2, & T \ll T_c. \end{cases} \quad (29)$$

For μ_{str} we cannot use the low- T asymptote of Eq. (25) since this limit for $g=0$ is different from that for $g>0$, see Eq. (B11). From the latter equation we find

$$\mu_{str} = \begin{cases} -f^2/6T - T \ln 4, & f/T \ll 1, \\ -f/2 - T \ln 2, & f/T \gg 1. \end{cases} \quad (30)$$

From equating the adsorption and stretching free energies the limiting forms of $f_{tr}(T)$ are found:

$$f_{tr} \approx \begin{cases} \frac{5 + \sqrt{5}}{2}(1 - T/T_c)\sqrt{T/T_c}, & T \approx T_c, \\ 2, & T \ll T_c. \end{cases} \quad (31)$$

The phase diagram for a zigzag chain is given in Fig. 14, both in the form $f(T/T_c)$ (a) and as $u(\chi)$ (b). The solid curves

were calculated from Eqs. (B10) and (C1)–(C4) for $g=0$, the asymptotes are given in Eq. (31) or take the simple form $u = 2\chi$ (b), see below. The most important difference with the previous cases is that f_{tr} does not depend on T in the low- T limit, so there is no re-entrance with decreasing temperature at a fixed force. The physical background is the following.

For a fully stretched zigzag chain the stretching parameter ζ equals $\frac{1}{2}$ because half of the steps are parallel to the surface. The entropy of such a stretched chain is not zero since the conformation is a meander line with four choices per two consecutive steps: $S_{str} = \ln 2$. This is exactly the same value as S_{ads} , because a $2d$ zigzag chain has two choices per step: either left or right. The low- T limit of the coexistence condition can be written by generalizing the argument discussed at the end of Sec. II. The chemical potentials (in units ε) are $\mu_{ads} = -1 - TS_{ads}$ and $\mu_{str} = -\zeta f - TS_{str}$, which gives

$$\zeta f_{tr} = 1 + T(S_{ads} - S_{str}). \quad (32)$$

Since the two entropic contributions are exactly the same, the low- T slope of the detachment force is zero and its limiting value is $f_{tr} = 2$, consistent with Eq. (31). Hence, the dependence $f_{tr}(T)$ is monotonic and no re-entrance occurs at low temperature.

Returning to the coordinates $u = f\ell/kT$ and $\chi = \varepsilon/kT$, the detachment curve in the strong adsorption limit takes the form

$$\zeta u_{tr} = \chi + (S_{ads} - S_{str}). \quad (33)$$

For the zigzag model this reduces to $u_{tr} = 2\chi$, which is the asymptote shown in Fig. 14(b). We conclude that the value of the intercept of the asymptotic straight line $u_{tr}\chi$ can be used as a criterion that defines whether re-entrance occurs: re-entrance requires a positive intercept.

VII. CONCLUDING REMARKS

We have analyzed in this paper the temperature dependence of the force needed to detach an infinitely long adsorbed polymer chain. For ideal walks on regular lattices exact expressions for the partition functions with and without an external force are available, so that a complete picture of all relevant thermodynamic quantities is obtained. There is a critical value of the detachment force f_{tr} at which a polymer chain desorbs in a first-order phase transition.

The central feature is the force-temperature phase diagram, in which the detachment curve $f_{tr}(T)$ defines the transition(s) between adsorbed and desorbed (stretched) states. For most lattice models $f_{tr}(T)$ displays a maximum. This implies that at a some constant force and with decreasing temperature the chain is first desorbed, then adsorbed in some temperature window, and then desorbed again. Therefore the stretched state is re-entered. We discussed the temperature dependence of the energy and the heat capacity upon cooling within and outside the adsorption window.

We analyzed long-range excluded-volume effects on the shape of the phase diagram. For temperatures just below the critical temperature T_c the detachment force scales as $f_{tr} \sim T^{1-\nu}(1 - T/T_c)^{\nu/\phi}$, and we also estimated the numerical prefactor for SAWs on a simple cubic lattice.

To take into account the steric repulsion of the neighboring monomers along the chain we used a simple model where immediate step reversals are forbidden. These analytical predictions were compared to recent MC simulations for SAWs (Refs. 11 and 13) on the same lattice. The MC data of Ref. 13 are rather inaccurate for temperatures close to the critical adsorption temperature T_c , as evaluated independently in other studies. However, when the data are replotted as f_{tr} versus T/T_c , the results for the analytical five-choice model and SAWs are very close.

We also discussed the effect of chain stiffness on the shape of the phase diagram, using correlated walks on a lattice. For very stiff chains the critical temperature T_c increases linearly with the Kuhn length A , the (negative) slope of the detachment line close to critical point is independent of A , and the (positive) low-temperature slope decreases as $1/A$. As a result, the range of forces where re-entrance occurs narrows. We conclude that a re-entrant (T, f) phase diagram is the general situation for lattice models. We found only one exception: a zigzag chain where both forward and back steps are forbidden does not show re-entrance.

In the coordinates $u = fl/kT$ and $\chi = \varepsilon/kT$ the coexistence curve $u_{tr}(\chi)$ is always monotonic. It approaches a straight line at large χ (strong adsorption). The intercept of this straight line can be used as a criterion that defines whether re-entrance occurs upon decreasing the temperature at constant force. Re-entrance is found only when the intercept of the asymptotic straight line $u_{tr}(\chi)$ is positive.

In conclusion we put forward two questions:

- (1) Does the re-entrance effect exist in off-lattice models, for example in the Grest–Kremer model,⁴¹ or in more realistic models of polymer chains?
- (2) What is the influence of stiffness on the re-entrance effect for nonideal chains?

We know of only one paper⁴² on mechanical desorption using MD simulations according to the Grest–Kremer model. Although the simulation data were not analyzed using (f, T) independent parameters, the intercept of the limiting straight line $u_{tr}(\chi)$ seems to be negative, so we conclude that this model does not show a re-entrant phase diagram. For the moment, it is an open question whether this applies to all off-lattice models.

The second question was not investigated systematically, except for a single publication of Kierfeld reporting MC simulations¹⁴ for stiff and relatively short chains, containing 100 monomer units but only two to five Kuhn segments. The phase diagram for these chains is similar to Fig. 13 for lattice chains, but it is steeper around the critical temperature. We suggest that in this region finite-size effects are important. Calculations for longer chains would be needed to resolve this issue.

Finally, we return to the analogy between the unzipping of DNA and the mechanical desorption of a polymer chain, as mentioned in the introduction. We speculate on the importance of the re-entrance effect in (T, f) coordinates for force-induced DNA denaturation. It is well known that double-stranded native DNA is quite stiff, with a persistence length close to 50 nm (so the Kuhn length is ~ 100 nm).⁴³ There-

fore, one could expect that its entropy in the fully bound state is rather small compared to a single strand completely adsorbed on a solid surface. In the unzipped state a single DNA strand is flexible: its typical Kuhn length is close to 1.5 nm.^{44,45} It was demonstrated experimentally by AFM (Refs. 46 and 47) that strong deformation of flexible chains is very well described by the Langevin formula.⁴⁸ This implies that the conformation-dependent entropy of the chain backbone tends to zero upon approaching the fully stretched state. Probably, in the low-temperature limit ΔS vanishes and according to the general thermodynamic relation [Eqs. (32) and (33)] the re-entrance effect for mechanical unzipping of double-stranded DNA is either nonexistent or at best very small. On the other hand, in the mechanical desorption of a single DNA strand from a solid adsorbing surface the entropy of the fully adsorbed state is likely to be quite considerable, which then would lead to re-entrance.

ACKNOWLEDGMENTS

A.M.S. acknowledges financial support from the Dutch National Science Foundation (NWO) through the joint project 047.017.026 “Polymers in nanomedicine: design, synthesis, and study of interpolymer and polymer-virus complexes in search of novel pharmaceutical strategies” and partial support from the Russian Foundation for Basic Research (RFBR Grant No. 08-03-00402-a). We are grateful to Ekaterina Zhulina and Alexei Polotsky for being able to use their unpublished results in Appendix A.

APPENDIX A: ADSORPTION AND STRETCHING FREE ENERGY FROM THE GRAND CANONICAL ENSEMBLE

Rubin¹⁷ derived the relation between the free energy and the adsorption energy for a lattice chain in the absence of a force, in the limit $N \rightarrow \infty$. His procedure may be generalized to include the effect of a force f acting on the end point as well, giving rise to an elastic energy contribution.

Like Rubin, we consider a grand canonical (gc) ensemble, where the length of the chain, as well as the lengths of trains and loops and the (one) tail are fluctuating. We need the statistical weights related to the free energy μ (with respect to a rod), to the adsorption energy $-\varepsilon$, and to the deformation energy $-f\ell$. We define those statistical weights as

$$\lambda = e^{-\tilde{\mu}}, \quad q = e^{\chi}, \quad z = e^u, \quad (\text{A1})$$

where $\tilde{\mu} = \mu/kT$, $\chi = \varepsilon/kT$, and $u = f\ell/kT$. The parameters λ and q take their lowest values λ_c and q_c in the critical point. On a simple cubic lattice $\lambda_c = 6$ and $q_c = 6/5$ for a six-choice walk, $\lambda_c = 5$ and $q_c = 5/4$ for a five-choice walk (no back step), and $\lambda_c = 4$ and $q_c = \sqrt{5} - 1$ for a four-choice walk (zigzag chain). The weights λ , q , and z enter the partition functions Q_s , Q_l , and Q_t for a train, a loop, and the (one) tail, respectively, consisting of n units. The gc partition functions for trains, loops, and the tail become:

$$\Xi_s(\lambda, q) = \sum_{n=1}^{\infty} Q_s(\lambda, q) \lambda^{-n}, \quad \Xi_t(\lambda) = \sum_{n=1}^{\infty} Q_t(\lambda) \lambda^{-n}, \quad (\text{A2})$$

$$\Xi_t(\lambda, z) = \sum_{n=1}^{\infty} Q_t(\lambda, z) \lambda^{-n}.$$

A tethered chain has always a train at the beginning, a tail at the end, and an alternation of loops and trains in between. Hence, the gc partition function of the chain as a whole has the form

$$\Xi = \Xi_s \Xi_t [1 + \Xi_s \Xi_t + (\Xi_s \Xi_t)^2 + \dots] = \frac{\Xi_s \Xi_t}{1 - \Xi_s \Xi_t}. \quad (\text{A3})$$

From the generating function method it is well known that the chemical potential is defined as the simple pole of Ξ . Hence, at any q and/or z the corresponding value of λ is found as the solution of the equation

$$\frac{1}{\Xi(\lambda, q, z)} = \frac{1 - \Xi_s(\lambda, q) \Xi_t(\lambda)}{\Xi_s(\lambda, q) \Xi_t(\lambda, z)} = 0. \quad (\text{A4})$$

The solution of $\Xi_s \Xi_t = 1$ gives λ_{ads} of the adsorbed state, and the solution of $1/\Xi_t = 0$ provides λ_{str} of the stretched state; the equilibrium situation corresponds to $\lambda = \max(\lambda_{\text{ads}}, \lambda_{\text{str}})$. In the stretched state λ_{str} does not depend on the adsorption energy.

Below, we restrict ourselves to a simple cubic lattice. Rubin derived Ξ as a function of λ and q , without giving explicit expressions for the partial contributions Ξ_s and Ξ_t . However, these are easily derived using his general procedure, and we can extend this procedure to also find $u(\lambda)$.

1. Six-choice walk

The train contribution is

$$\Xi_s = (q/\lambda) [1 + 4q/\lambda + (4q/\lambda)^2 + \dots] = \frac{1}{\lambda/q - 4}. \quad (\text{A5})$$

In the critical point, where $\lambda_c/q_c = 5$, $\Xi_s = 1$. For high λ ($\Xi_s \rightarrow \infty$) we have $\lambda = 4q$.

The loop contribution may be written as

$$\Xi_t = e^{-\text{acosh } y} = y - \sqrt{y^2 - 1}, \quad y = \frac{1}{2}(\lambda - 4). \quad (\text{A6})$$

In the critical point ($\lambda_c = 6$) $y = 1$ and $\Xi_t = 1$, and $\Xi_t = 1/2y = 1/\lambda$ for high λ where Ξ_t goes to zero.

The tail partition function Ξ_t in the presence of a force was derived by Zhulina (unpublished results):

$$\Xi_t = \frac{\Xi_t}{e^{-u} - \Xi_t}. \quad (\text{A7})$$

In the adsorption region ($\lambda = e^{-\tilde{\mu}_{\text{ads}}}$) Eq. (A4) in the form $1/\Xi_s = \Xi_t$ gives the relation between q and λ :

$$q = \frac{\lambda}{\lambda/2 + 2 - \sqrt{(\lambda/2 - 2)^2 - 1}}, \quad \lambda = \frac{p}{\sqrt{3 + p - 2}}, \quad (\text{A8})$$

$$p = \frac{q}{q - 1}.$$

With $\tilde{\mu}_{\text{ads}} = -\ln \lambda$, the second form is Eq. (1) of the main paper.

In the desorption region $\lambda = e^{-\tilde{\mu}_{\text{str}}}$. From Eq. (A4) in the form $1/\Xi_t = 0$ we find with Eq. (A7) $u = \text{acosh } y$. Hence, $y = \cosh u$ or $\lambda = 4 + 2 \cosh u$, which gives Eq. (4) of the main paper.

The detachment curve is found from $\mu_{\text{ads}} = \mu_{\text{str}}$, or $4 + 2 \cosh u = p/(\sqrt{3 + p - 2})$, which may be rewritten as $2 + e^{-u} = \sqrt{3 + p}$. This leads to Eq. (5) of the main paper.

2. Four-choice walk (zigzag chain)

Expressions for Ξ_s and Ξ_t have been derived by Polotsky (unpublished results). The train contribution is

$$\Xi_s = \frac{4}{\lambda} \frac{q^2}{\lambda - 2q}. \quad (\text{A9})$$

In the critical point $\Xi_s = 1$ and $\lambda_c = 4$, so q_c follows as $\sqrt{5} - 1$. For high λ ($\Xi_s \rightarrow \infty$) $\lambda = 2q$.

The loop contribution may be written in the same way as Eq. (A6), but with a different form for the parameter y :

$$\Xi_t = e^{-\text{acosh } y} = y - \sqrt{y^2 - 1}, \quad y = \frac{1}{8}\lambda(\lambda - 2). \quad (\text{A10})$$

Again we have $y = 1$ in the critical point, but now $y = \lambda^2/8$ and $\Xi_t = 1/2y = 4/\lambda^2$ for large λ . From $1/\Xi_s = \Xi_t$ we find the relation between y (or λ) and q :

$$2q^2(y - \sqrt{y^2 - 1}) + (q - 1)(1 + \sqrt{1 + 8y}) - 4y = 0. \quad (\text{A11})$$

This relation is identical to an earlier result derived by Rubin,¹⁸ who used the form $2/q^2 - t/q + t/2 - 1 + \sqrt{(1-t)(1+t^2/4 + t^3/4)} = 0$, with $t = 4/\lambda$. Equation (A11) gives an explicit form $q(\lambda)$ by solving the quadratic equation in q . A closed solution for $y(q)$ or $\lambda(q)$ is possible but complicated, since Eq. (A11) is quartic in y .

At the critical point ($y = 1$) we find again $q_c = \sqrt{5} - 1$. For high λ Eq. (A11) reads $q\lambda - \lambda^2/2 = 0$ or $\lambda = 2q$, the same result as followed from Eq. (A9).

In the desorption region we can again use Eq. (A7): $\cosh u = y$, which now gives

$$\cosh u = \frac{1}{8}\lambda(\lambda - 2) \quad \lambda = 1 + \sqrt{1 + 8 \cosh u}. \quad (\text{A12})$$

This relation may also be derived from the transfer matrix [Appendix B, Eq. (B10) with $g = 0$].

The detachment curve is obtained by using the same λ in Eqs. (A11) and (A12). An explicit solution $u(q)$ or $q(u)$ is cumbersome, but the solution is easily found parametrically: for given λ we calculate q from Eq. (A11) and the corresponding u from Eq. (A12). Asymptotic forms for λ close to 4 and for large λ are easily obtained as $u(q)$ or $u(\lambda)$, which in the main paper [Eq. (31)] is translated toward $f(T)$.

3. Five-choice walk (no back step)

Also for this case Polotsky derived the partition functions for trains and loops. The train part is

$$\Xi_s = \frac{4}{\lambda} \frac{q^2}{\lambda - 3q}. \quad (\text{A13})$$

In the critical point ($\lambda_c=5$) we have $q_c=5/4$, and $\lambda=3q$ for high λ .

The loop contribution is slightly more complicated than in Eqs. (A6) and (A10):

$$\Xi_l = \sqrt{\frac{5}{4} \frac{\lambda}{\lambda + 1}} (y - \sqrt{y^2 - 1}), \quad (\text{A14})$$

$$y = \frac{\sqrt{5} \lambda^4 - 3\lambda^3 - \lambda^2 - 5\lambda - 4}{16 \lambda \sqrt{\lambda(\lambda + 1)}}.$$

Unlike in the previous cases the parameter y is not exactly unity in the critical point: $y_c = \sqrt{(2401/2400)} = 49/(20\sqrt{6})$. That is why there is now a prefactor $\sqrt{(5/4)\lambda/(\lambda+1)}$, which varies from $\sqrt{(25/24)}$ in the critical point to $\sqrt{(5/4)}$ for high λ . For large λ we have $y = (\sqrt{5}/16)\lambda^2$ and $\Xi_l = \sqrt{5}/y = (4/\lambda)^2$.

From $1/\Xi_s = \Xi_l$ we obtain the relation between q and λ :

$$(\lambda/q)^2 - 3(\lambda/q) - 4\Xi_l = 0. \quad (\text{A15})$$

A closed solution for $\lambda(q)$ does not exist, but the inverse relation $q(\lambda)$ is easy by solving the quadratic equation in $1/q$. At the critical point ($\Xi_l=1$) we have $\lambda_c/q_c=4$, for high λ Eq. (A15) reduces to $(\lambda/q)^2 - 3(\lambda/q) = 0$ or $\lambda=3q$, as found above.

For a five-choice walk no solution for Ξ_l is known; Eq. (A7) does not apply. However, the relation between λ and u may be derived from the transfer matrix [see Appendix B, Eq. (B10) with $g=1$]:

$$\cosh u = \frac{\lambda^2 - 4\lambda + 5}{2\lambda}. \quad (\text{A16})$$

The detachment curve is again found parametrically, by calculating q from Eq. (A15) and u from Eq. (A16) for given λ . Explicit asymptotic forms for λ close to 5 and for large λ are available; they are given in the main paper [Eq. (18)] in the form $f(T)$.

APPENDIX B: STRETCHING FREE ENERGY FOR CHAINS WITH AND WITHOUT STIFFNESS

The stretching free energy is easily calculated from the transfer matrix. The method is based upon recurrence equations expressing the partition function $Z(N+1)$ for $N+1$ particles (or steps) in terms of $Z(N)$. The method was first introduced in the context of the 1d Ising model with nearest-neighbor interactions.⁴⁹ Because of the close analogy with ideal walks with short-range correlations on a lattice, this matrix method can be applied also for evaluating the partition function of stretched lattice chains.

We first consider a random walk on a simple cubic lattice in the presence of a dipolar orienting field equivalent to the dimensionless end-force $u=f\ell/kT$ directed away from

the surface. Steps parallel to the field are assigned a weight e^u , antiparallel steps have a weight e^{-u} , and steps normal to the field have weight unity.

We introduce a vector $\mathbf{Z}(N)$ of restricted partition functions with three components $Z_i(N)$, where i indicates the direction of the last step: parallel ($i=1$), normal ($i=2$), or antiparallel ($i=3$) to the field. The recurrence equations for a random walk are as follows:

$$\begin{aligned} Z_1(N+1) &= e^u[Z_1(N) + Z_2(N) + Z_3(N)], \\ Z_2(N+1) &= 4[Z_1(N) + Z_2(N) + Z_3(N)], \\ Z_3(N+1) &= e^{-u}[Z_1(N) + Z_2(N) + Z_3(N)]. \end{aligned} \quad (\text{B1})$$

The factor 4 in the middle equation represents the four choices for steps normal to the field.

Equation (B1) may be written more compactly in matrix form:

$$\mathbf{Z}(N+1) = \mathbf{T}\mathbf{Z}(N), \quad (\text{B2})$$

where the transfer matrix \mathbf{T} is given by

$$\mathbf{T} = \begin{pmatrix} e^u & e^u & e^u \\ 4 & 4 & 4 \\ e^{-u} & e^{-u} & e^{-u} \end{pmatrix} \quad (\text{B3})$$

When we start from $N=1$ Eq. (B2) reads

$$\mathbf{Z}(N+1) = \mathbf{T}^N \mathbf{Z}(1). \quad (\text{B4})$$

For large N the precise form of $\mathbf{Z}(1)$ does not matter: $Z_i(1)=1$ for any i is adequate. According to standard matrix algebra $Z(N) = \sum_i Z_i(N)$ can be written in terms of the three eigenvalues λ_i of the matrix \mathbf{T} :

$$Z(N+1) = \sum_{i=1}^3 \lambda_i^N. \quad (\text{B5})$$

The eigenvalues are found from the characteristic equation resulting from setting the determinant of $\mathbf{T} - \lambda\mathbf{I}$ (where \mathbf{I} is the identity matrix) zero:

$$|\mathbf{T} - \lambda\mathbf{I}| = 0. \quad (\text{B6})$$

In our case the characteristic equation is cubic in λ .

For large N the sum in Eq. (B5) is dominated by the largest eigenvalue λ_{\max} :

$$Z(N) = \lambda_{\max}^N. \quad (\text{B7})$$

The free energy per step is given by $\tilde{\mu} = -N^{-1} \ln Z = -\ln \lambda_{\max}$. Henceforth, we omit the subscript max, so $\lambda = e^{-\tilde{\mu}}$ has the same meaning as in Appendix A [Eq. (A1)].

In the absence of a force $e^u = e^{-u} = 1$. The characteristic equation for Eq. (B3) in this form then gives $\lambda^2(\lambda-6)=0$, so $\lambda=6$ and $\tilde{\mu} = \tilde{\mu}_0 = -\ln 6$, as used in Eq. (1) of the main paper. When $u \neq 0$, Eq. (B6) takes the form $\lambda^2(4+2 \cosh u - \lambda) = 0$. Hence, $\lambda = 4 + 2 \cosh u$, which was also found from Appendix A 1 and immediately leads to Eq. (4) of the main paper.

In this formalism, it is now very easy to ascribe different statistical weights to certain steps; now the walk is no longer random. We can also include a stiffness parameter g . For example, when immediate step reversals are eliminated and a

forward step (i.e., in the direction of the previous step) carries a weight g , the recurrence relations [Eq. (B1)] are modified, leading to the following transfer matrix:

$$\mathbf{T} = \begin{pmatrix} ge^u & e^u & 0 \\ 4 & 2+g & 4 \\ 0 & e^{-u} & ge^{-u} \end{pmatrix} \quad (\text{B8})$$

The characteristic equation is

$$\lambda^3 - (2+g+2g \cosh u)\lambda^2 + [g^2 + 2(g^2 + 2g - 4)\cosh u]\lambda + g(8 - 2g - g^2) = 0 \quad (\text{B9})$$

or

$$\cosh u = \frac{1}{2\lambda} \frac{g^3 - (g^2 + \lambda^2)(\lambda - 2) + g(\lambda^2 - 8)}{g^2 - g(\lambda - 2) - 4}. \quad (\text{B10})$$

A closed form $\lambda(u)$ for given g is possible, but too cumbersome to write out. The special cases $g=0$ (zigzag chain) and $g=1$ (no back step) have already been discussed in Appendix A.

Equation (B10) has the following limits:

$$\lambda \approx \begin{cases} \lambda_c [1 + (A/6)u^2], & \lambda \approx \lambda_c, \\ ge^u, & \lambda \gg \lambda_c, g > 0, \\ 2e^{u/2}, & \lambda \gg \lambda_c, g = 0, \end{cases} \quad (\text{B11})$$

where the critical value of λ and the Kuhn length A (in units ℓ) are defined as

$$\lambda_c = 4 + g, \quad A = 1 + g/2. \quad (\text{B12})$$

We used these asymptotic forms in the main paper to obtain $\mu_{\text{sur}}(T)$ [Eq. (30) for $g=0$, Eq. (17) for $g=1$, and Eq. (25) for arbitrary g].

Equation (B10) gives the relation between u and λ for arbitrary g . In order to find the detachment curve we need also the relation between q and λ . We discuss that relation in Appendix C.

APPENDIX C: ADSORPTION FREE ENERGY FOR CHAINS OF ARBITRARY STIFFNESS

A strict theory for the adsorption of lattice chains with arbitrary stiffness on a solid plane was presented by Birshstein *et al.*,³¹ for a simple cubic lattice where the back step was forbidden. Chain stiffness was introduced by assigning a statistical weight g to a forward step, in the direction of the previous step. Four steps perpendicular to previous step have a statistical weight unity. Attachment to the surface results in a statistical weight $q=e^\chi$. As shown before [Eq. (A8)], a convenient parameter is $p=q/(q-1)$ instead of q .

The chemical potential of a chain (counted from a rod) is $\bar{\mu} = \min(\bar{\mu}_0, \bar{\mu}_{\text{ads}})$ where $\bar{\mu}_0 = -\ln \lambda_c = -\ln(4+g)$ and $\bar{\mu}_{\text{ads}} = -\ln \lambda$, and $\lambda = \lambda(g, p)$ is the maximal root of the equation:

$$Ap^2 + Bp + C = 0, \quad (\text{C1})$$

where A , B , and C are a function of λ and g as follows:

$$A = 1 - x_5 - x_8,$$

$$B = (x_1x_8 + x_5x_4) - (x_2x_7 + x_3x_6) - (x_1 + x_4), \quad (\text{C2})$$

$$C = x_1x_4 - x_2x_3.$$

The coefficients x_i depend on λ and g . In the equations below we use the abbreviations $a = \lambda - g$, $b = \lambda - g - 2$, $c = ab - 4$, and $d = gb + 4$.

$$x_1 = \lambda c Y_0 - d Y_1, \quad x_2 = \lambda a Y_0 + \lambda Y_1,$$

$$x_3 = 4\lambda a Y_0 - 4g Y_1, \quad x_4 = \lambda a^2 Y_0 - 2\lambda g Y_1, \quad (\text{C3})$$

$$x_5 = -gc Y_0 - gb Y_1, \quad x_6 = -c Y_0 - b Y_1,$$

$$x_7 = -4ag Y_0 - 4g Y_1, \quad x_8 = -4a Y_0 - 4 Y_1,$$

where Y_0 and Y_1 are defined as

$$Y_0 = \frac{1}{\sqrt{P}\sqrt{P+4\lambda d}}, \quad Y_1 = \frac{Y_0 P - 1}{2d}, \quad P = a(c-4). \quad (\text{C4})$$

Equation (C1) provides for any g the relation $p(\lambda)$, which is easily converted toward $q(\lambda)$. Combining this with $u(\lambda)$ as given in Eq. (B9) allows the calculation of the detachment curve for arbitrary g .

For interpreting the trends, it is useful to have limiting forms of the complicated equations above. We first consider the critical point, where λ_c and q_c take their lowest values. Clearly, $\lambda_c = 4 + g$, see Eq. (B12). The critical value q_c depends on g as follows:

$$q_c = \frac{2\lambda_c}{\lambda_c - 2 + \sqrt{(\lambda_c - 2)^2 + 16}} = \frac{2(A+1)}{A + \sqrt{A^2 + 4}}, \quad (\text{C5})$$

where $A = 1 + g/2$ [Eq. (B12)]. The critical value χ_c follows as $\mu_c = \ln q_c$. For very stiff chains $q_c = 1 + 1/A$ and $\chi_c = 1/A$.

The asymptotic forms $\lambda(q)$ for arbitrary g can now be written as

$$\lambda = \begin{cases} \lambda_c \left\{ 1 + \frac{\lambda_c^2 A^2 + 4}{q_c^2 12A} (\chi - \chi_c)^2 \right\}, & \lambda \approx \lambda_c, \\ (2+g)q, & \lambda \gg \lambda_c, \end{cases} \quad (\text{C6})$$

These limits, in the form $\mu_{\text{ads}}(T)$, have been used in the main paper [Eq. (29) for $g=0$, Eq. (16) for $g=1$, and Eq. (25) for arbitrary g].

¹D. Poland and H. A. Sheraga, *Theory of Helix-Coil Transitions in Biopolymers* (Academic, New York, 1970).

²A. Kornberg and T. Baker, *DNA Replications*, 3rd ed. (Freeman, New York, 1992).

³S. M. Bhattacharjee, *J. Phys. A* **33**, L423 (2000).

⁴B. Essevez-Roulet, U. Bockelman, and F. Heslot, *Proc. Natl. Acad. Sci. U.S.A.* **94**, 11935 (1997).

⁵S. Kumar, J. Jensen, J. L. Jacobsen, and A. J. Guttmann, *Phys. Rev. Lett.* **98**, 128101 (2007).

⁶F. Hanke, L. Livadaru, and H. J. Kreuzer, *Europhys. Lett.* **69**, 242 (2005).

⁷A. M. Skvortsov, A. A. Gorbunov, E. B. Zhulina, and T. M. Birshstein, *Vysokomolekularnye Soedineniya seriya A* **A20**, 278 (1978).

⁸A. A. Gorbunov and A. M. Skvortsov, *J. Chem. Phys.* **98**, 5961 (1993).

⁹A. M. Skvortsov, A. A. Gorbunov, and L. I. Klushin, *J. Chem. Phys.* **100**, 2325 (1994).

- ¹⁰L. I. Klushin, A. M. Skvortsov, and A. A. Gorbunov, *Phys. Rev. E* **56**, 1511 (1997).
- ¹¹J. Krawczyk, T. Prellberg, A. L. Owczarek, and A. Rechnitzer, *J. Stat. Mech.: Theory Exp.* P10004 (2004).
- ¹²J. Krawczyk, A. L. Owczarek, T. Prellberg, and A. Rechnitzer, *J. Stat. Mech.: Theory Exp.* P05008 (2005).
- ¹³P. K. Mishra, S. Kumar, and Y. Singh, *Europhys. Lett.* **69**, 102 (2005).
- ¹⁴J. Kierfeld, *Phys. Rev. Lett.* **97**, 058302 (2006).
- ¹⁵E. Orlandini, M. C. Tesi, and S. G. Whittington, *J. Phys. A* **37**, 1535 (2004).
- ¹⁶D. Marenduzzo, A. Trovato, and A. Maritan, *Phys. Rev. E* **64**, 031901 (2001).
- ¹⁷R. J. Rubin, *J. Chem. Phys.* **43**, 2392 (1965).
- ¹⁸R. J. Rubin, *J. Res. Natl. Bur. Stand., Sect. B* **69**, 3001 (1965).
- ¹⁹R. J. Rubin, *J. Res. Natl. Bur. Stand., Sect. B* **70**, 237 (1966).
- ²⁰P.-G. de Gennes, *Scaling Concepts in Polymer Physics* (Cornell University Press, Ithaca, 1979).
- ²¹T. W. Burkhardt, E. Eisenriegler, and I. Guim, *Nucl. Phys. B* **316**, 559 (1989).
- ²²H.-W. Diehl and M. Shpot, *Phys. Rev. Lett.* **73**, 3431 (1994).
- ²³H.-W. Diehl and M. Shpot, *Nucl. Phys. B* **528**, 595 (1998).
- ²⁴P. Grassberger, *J. Phys. A* **38**, 323 (2005).
- ²⁵H. Meirovitch and S. Livne, *J. Chem. Phys.* **88**, 4507 (1988).
- ²⁶M. Luo, *J. Chem. Phys.* **128**, 044912 (2008).
- ²⁷S. Bhattacharya, H.-P. Hsu, A. Milchev, V. G. Rostiashvili, and T. A. Vilgis, *Macromolecules* **41**, 2920 (2008).
- ²⁸A. M. Skvortsov, T. M. Birshtein, E. B. Zhulina, and A. A. Gorbunov, *J. Pol. Sci. (Russia)* **A18**, 2097 (1976).
- ²⁹R. Kubo, *Statistical Mechanics: An Advanced Course with Problems and Solutions* (North-Holland, Amsterdam, 1965).
- ³⁰J. des Cloizeaux and G. Jannink, *Polymers in Solutions: Their Modeling and Structure* (Clarendon, Oxford, 1990).
- ³¹T. M. Birshtein, E. B. Zhulina, and A. M. Skvortsov, *Biopolymers* **18**, 1171 (1979).
- ³²T. Vrbová and K. Prochazka, *J. Phys. A* **32**, 5469 (1999).
- ³³H. P. Hsu and P. Grassberger, *Eur. Phys. J. B* **36**, 209 (2003).
- ³⁴M. Fisher, *J. Chem. Phys.* **44**, 616 (1966).
- ³⁵E. G. Timoshenko, Y. A. Kuznetsov, and R. Connolly, *J. Chem. Phys.* **116**, 3905 (2002).
- ³⁶P. Pincus, *Macromolecules* **9**, 386 (1976).
- ³⁷P. Grassberger, *J. Phys. A* **26**, 2769 (1993).
- ³⁸R. Hegger and P. Grassberger, *J. Phys. A* **27**, 4069 (1994).
- ³⁹Y. C. Gong and Y. M. Wang, *Macromolecules* **35**, 7492 (2002).
- ⁴⁰E. J. J. van Rensburg and A. R. Rechnitzer, *J. Phys. A* **37**, 6875 (2004).
- ⁴¹G. K. Grest and K. Kremer, *Phys. Rev. A* **33**, 3628 (1986).
- ⁴²S. Bhattacharya, V. G. Rostiashvili, A. Milchev, and T. A. Vilgis, *Macromolecules* (unpublished).
- ⁴³W. H. Taylor and P. J. Hagerman, *J. Mol. Biol.* **212**, 363 (1990).
- ⁴⁴S. B. Smith, Y. Cui, and C. Bustamante, *Science* **271**, 795 (1996).
- ⁴⁵B. Maier, D. Bensimon, and V. Croquette, *Proc. Natl. Acad. Sci. U.S.A.* **97**, 12002 (2000).
- ⁴⁶N. B. Holland, T. Hugel, G. Neuert, A. Cattani-Scholz, C. Renner, D. Oesterhelt, L. Moroder, M. Seitz, and H. E. Gaub, *Macromolecules* **36**, 2015 (2003).
- ⁴⁷T. Hugel, M. Rief, H. E. Gaub, and R. R. Netz, *Phys. Rev. Lett.* **94**, 048301 (2005).
- ⁴⁸H. Yamakawa, *Modern Theory of Polymer Solutions* (Harper and Row, New York, 1971).
- ⁴⁹E. Ising, *Z. Phys. A* **31**, 253 (1925).